power-law shock wave," Prikl. Math. i Mekhan. **24**, 518 (1960); J. Appl. Math. and Mech. **24**, 756 (1960); see also Probstein, R. F., "Recent Soviet advances in inviscid hypersonic aerodynamics," Aerospace Eng. **20**, 10 (July 1961).

[7] Hayes, W. D., "On hypersonic similitude," Quart. Appl. Math. **5**, 105 (1947).

[8] Hayes, W. D. and Probstein, R. F., *Hypersonic Flow Theory* (Academic Press, New York, 1959).

[9] Bertram, M. H., "Viscous and leading-edge thickness effects on the pressure on the surface of a flat plate in hypersonic flow," J. Aeron. Sci. **21**, 430 (June 1954).

[10] Hammitt, A. G., Vas, I. E., and Bogdonoff, S. M., "Leading-edge effects on the flow over a flat plate at hypersonic speeds," Princeton Aeron. Eng. Rept. 326 (1955).

[11] Hammitt, A. G. and Bogdonoff, S. M., "Leading-edge effect on the flow over a flat plate," Jet Propulsion **26**, 241 (May 1956).

[12] Creager, M. O., "Effects of leading-edge blunting on the local heat transfer and pressure distribution over flat plates in supersonic flow," NACA TN4142 (Dec. 1957).

[13] Cheng, H. K., "Hypersonic flow with leading-edge bluntness and boundary layer displacement effects," ONR-Sponsored Cornell Aeron. Lab. Rept. AF 1285-A-4 (Aug. 1960).

[14] Cheng, H. K., Hall, J. G., Golian, T. C., and Herzberg, A., "Boundary-layer displacement and leading-edge bluntness effects in high-temperature hypersonic flow," J. Aerospace Sci. **28**, 353 (May 1961).

[15] Mirels, H. and Thornton, P. R., "Effects of body perturbations on hypersonic flow over slender, power-law bodies," NASA TR R-45 (May 1959).

[16] Van Dyke, M. D., "Application of hypersonic small-disturbance theory," J. Aeron. Sci. **21**, 179 (March 1954); also NACA TR 1194 and NACA TN 3173.

[17] Lees, L., "Laminar heat transfer over blunt-nosed bodies at hypersonic flight speeds," Jet Propulsion **26**, 259 (April 1956).

[18] Oguchi, H., "The sharp leading edge problem in hypersonic flow," *Rarefied Gas Dynamics*, edited by L. Talbot (Academic Press, New York, 1961); see also Brown University Rept., ARL TN 60-133 (Aug. 1960).

[19] Kubota, T., "Investigation of flow around simple bodies in hypersonic flow," GALCIT Memo. 40 (June 1957).

[20] Sedov, L. I., *Similarity and Dimensional Methods in Mechanics* (Gostekhizdat, Moscow, 1957), 4th ed.; transl. edited by M. Holt (Academic Press, New York, 1959).

[21] Sakurai, A., "On the propagation and structure of the blast wave—part I," J. Phys. Soc. (Japan) **9**, 256 (March-April 1954).

[22] Lin, S. C., "Cylindrical shock wave produced by instantaneous energy release," J. Appl. Phys. **25**, 54 (Jan. 1954).

[23] Hall, J. G. and Golian, T. C., "Shock-tunnel studies of hypersonic flat-plate airflows," Cornell Aeron. Lab. Rept., AD-1052-A-10 (Dec. 1960).

[24] Oguchi, H., "First-order approach to a strong interaction problem in hypersonic flow over an insulated flat plate," University of Tokyo, Aeron. Res. Inst. Rept. 330 (June 1958).

FEBRUARY 1963 AIAA JOURNAL VOL. 1, NO. 2

Some Applications of Detailed Wind Profile Data to Launch Vehicle Response Problems

HOMER G. MORGAN* AND DENNIS F. COLLINS JR.*

NASA Langley Research Center, Hampton, Va.

The response of a launch vehicle to a number of detailed wind profiles has been determined. The wind profiles were measured by two techniques that are described briefly. One of these techniques uses an angle-of-attack sensor in conjunction with guidance data to measure the wind profile traversed by some particular launch vehicle. The other wind-measuring technique is a photographic triangulation method, whereby two cameras take simultaneous pictures of a vertical trail of smoke left by a launch vehicle or sounding rocket. The response of a vehicle flying these detailed profiles is compared with the response of the same vehicle flying through balloon-measured profiles. The response to the detailed wind profiles, relative to the balloon-measured profiles, is characterized by the large excitation of the rigid pitch and elastic bending modes. This is found to cause higher loads on the launch vehicle structure. Established design criteria that use balloon-measured wind profiles have accounted for this increased load arbitrarily by adding a load due to some type of discrete gust.

Nomenclature

M = bending moment, lb-in.
M_{detailed} = bending moment induced by a detailed wind profile, lb-in.
M_{limit} = limit bending moment, lb-in.
M_{smoothed} = bending moment induced by a balloon-type wind profile, lb-in.
V_a = relative airstream velocity, fps
V_i = inertial velocity, fps
V_w = wind velocity, fps
y = translation normal to a reference trajectory, in.
α = angle of attack, rad
γ = flight-path angle, rad
θ = attitude angle, rad

Presented at the ARS Launch Vehicles: Structures and Materials Conference, Phoenix, Ariz., April 3–5, 1962; revision received November 1, 1962.

* Aerospace Technologist.

Introduction

THE wind and gust criteria for determining design loads on launch vehicles and the analytical methods by which these criteria are applied reflect the characteristics of available wind and gust data. The wind data have been obtained primarily from balloon soundings that detect only the gross motion of the atmosphere and filter out the small-scale fluctuations as indicated in Fig. 1. Examples of design criteria based on such wind data are the synthetic wind profiles of Refs. 1–4 and the measured profiles in Refs. 3 and 5. Most of the gust data that have been available were for vertical gusts (or turbulence) measured by a horizontally flying airplane,[6–8] also

indicated in the figure. The gust velocities have been assumed isotropic, and criteria based on vertical gust data for application to horizontally flying vehicles (airplanes) have been adapted to vertically flying vehicles. Vehicle loads usually are predicted using a rigid-body variable coefficient analysis with the wind profile as a forcing function and an elastic-body fixed coefficient analysis with the gust as a forcing function. Total design loads then are found by combining loads from the two sources—winds and gusts. The shortcomings of these criteria and analytical techniques are well known, but improvements have awaited the availability of better wind and gust data.

Wind and gust data of an improved nature just now are becoming available. These data have been obtained by techniques that permit a better measurement of the continuous function of horizontal wind vs altitude, as described in Refs. 9–12. Although these data are too new and too meager for design criteria using them to have been established, the analytical techniques for predicting wind and gust loads must be reconsidered in view of the improved data.

In this paper a brief discussion of two of the methods for obtaining detailed wind profile data will be given. Wind data obtained by these methods then will be used to predict the loads and responses of a solid propellant launch vehicle. The loads are determined using a program that accounts for the elasticity of the booster as well as the varying coefficients of the differential equations. Comparisons are made with the loads that would have been predicted if the wind had been measured by a sounding balloon.

Detailed Wind Profile Data

Gusts and winds for application to vertically rising launch vehicles are differentiated only by their wavelengths. This distinction has been made primarily because of the form of available data. If data were available which described the motion of the atmosphere with enough detail, so that both the long and short wavelength variations were included, the wind and gust design criteria could be combined. Such data also are needed for the analysis of particular missile flights, either for evaluation of design criteria, for comparison of measured and calculated loads, or for failure investigations. In recent years, such data have begun to be collected by a number of methods. Two such techniques will be described briefly and examples of the data presented.

Angle-of-Attack Vane Method

The α-vane method, described in considerable detail in Ref. 9, makes use of sensor equipment carried routinely on many launch vehicles for guidance and control functions. A sketch of the measuring scheme is shown in Fig. 2, following Ref. 9, for the pitch plane only. Similar measurements in the yaw plane will determine the other component of wind. An initial assumption is made that the wind velocity V_w is horizontal. (As illustrated here, the wind is a headwind.) The vehicle's inertial velocity V_i, its flight-path angle γ, and its attitude angle θ are the quantities measured normally

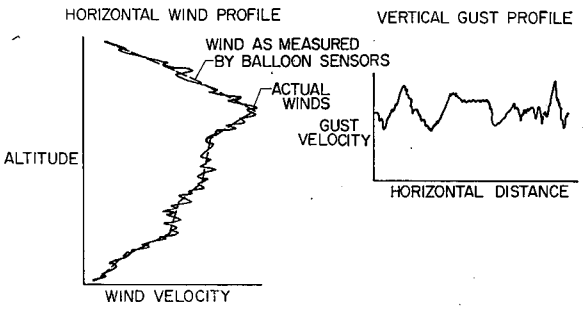

Fig. 1 Types of available wind and gust data

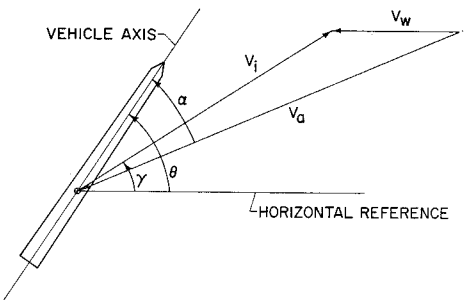

Fig. 2 Wind measurement using an angle-of-attack sensor

for guidance and control. An angle-of-attack sensor measures the angle α between the vehicle axis and the freestream velocity. This sensor is carried as part of the guidance and control equipment on some vehicles, or it may be added for this specific purpose. These measurements provide enough information to determine the wind velocity in whatever time or altitude increments are required, provided the data are continuous. Since winds measured by this technique are those experienced by the flight vehicle, these data especially are useful for loads analysis of the particular flight.

An example of data obtained by this method is presented in Fig. 3. These data, similar to those of Ref. 9, were obtained from W. W. Vaughan of Marshall Space Flight Center. For comparison, the wind profile as measured by a radiosonde balloon, released about 30 min after the vehicle launch, also is given. Only the lower altitude portions of the east-west components are presented, since these produce the principal loadings on a vehicle. Figure 3 shows the short wavelength variations in the α-vane wind profile which do not appear in the radiosonde balloon-measured profile (for example, at 25,000 ft altitude). It should be noted that the primary function of the instrumentation used to obtain these α-vane wind data was guidance and control, and the wind data were obtained only as a by-product. The α-vane data have been reduced to give a wind velocity in $\frac{1}{2}$-sec intervals of flight time. Since the flight velocity increases with altitude, the spread of altitude between velocity measurements also increases with altitude in this case. However, if the data exist in continuous form, these wind data points could be obtained in whatever increment is desired.

The particular advantage of the α-vane technique of wind measurement is that an instantaneous and continuous record of winds experienced by a particular missile is available. It would seem that this wind-measuring scheme would be employed whenever direct measurements of launch vehicle loads are attempted. The main disadvantage of this tech-

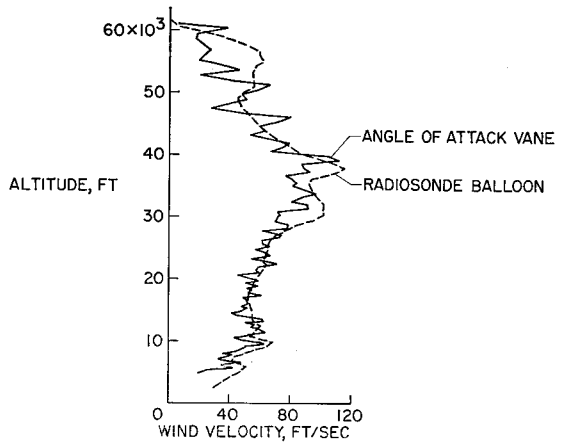

Fig. 3 Wind profiles measured using angle-of-attack sensors and radiosonde balloons

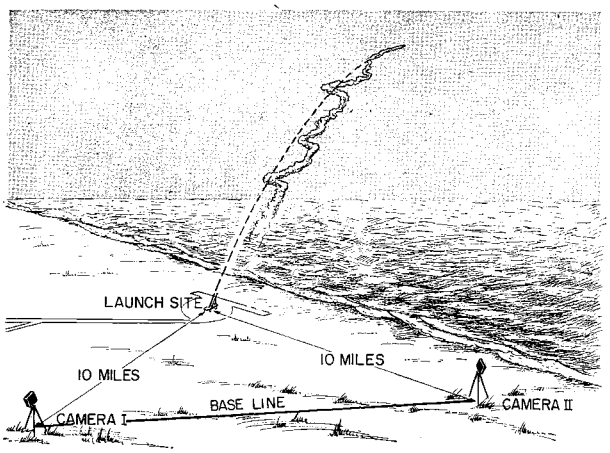

Fig. 4 Wind measurement by the smoke-trail method

nique is the accuracy and high-frequency response required of the instrumentation, particularly the angle-of-attack sensor. These requirements result in a very costly measurement scheme, usable for monitoring specific flights but not particularly attractive as a routine wind data collection system.

Smoke-Trail Method

The second technique of measuring detailed winds, the smoke-trail method, has been described in Refs. 10 and 11. A schematic diagram of the measurement setup is shown in Fig. 4. It is an optical-photographic method of deducing wind velocities by triangulation from two cameras taking photographs of a visible trail of smoke left by an ascending rocket. The smoke may be the visible exhaust trail left by some rockets or may be generated artificially by chemical releases into the airstream. The individual particles of smoke reach equilibrium with the atmosphere within seconds after the passage of the rocket. Two cameras, located about 10 miles from the launch site, take synchronized pictures of the trail in known time increments. Triangulation then is used on a set of these photographs to determine the position of points along the smoke trail, usually in 100-ft-altitude increments, although smaller increments are possible. Then, using position data from two sequential sets of pictures and the time interval between the pictures, the wind-velocity profile is found. All the data are obtained within about 2 min after the rocket is launched.

An example of the data obtained by the smoke-trail method from Ref. 10 is presented in Fig. 5. The winds measured on this particular day were low, less than 100 fps, but a measurement of velocity was obtained for each 100-ft

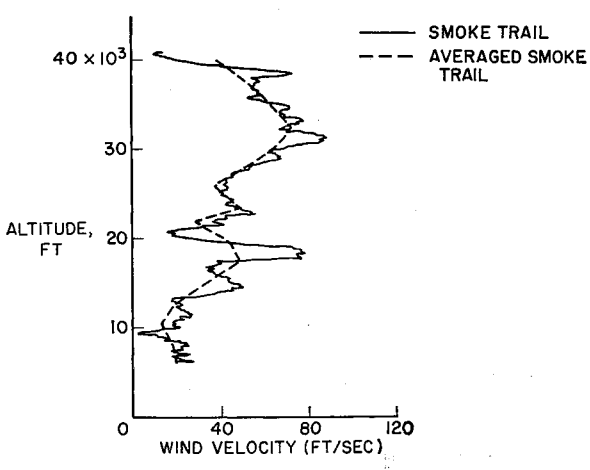

Fig. 5 Wind profiles measured by the smoke-trail method

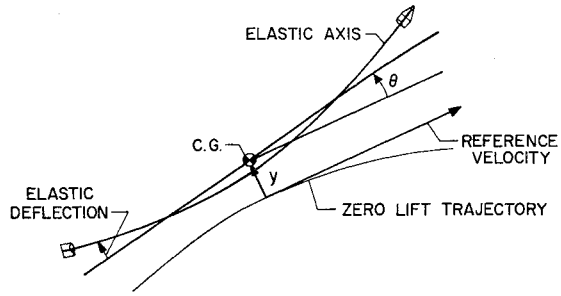

Fig. 6 Coordinate system used in the calculations

change in altitude. The short wavelength variations in wind velocity, or horizontal gusts, are very apparent.

For comparison, an averaged smoke-trail profile is presented in Fig. 5 also. These are smoke-trail data that have been averaged over 2000-ft-altitude increments, the same altitude increment usually used in reducing balloon data. It should be noted that this averaged profile is just one of many such profiles that could be obtained from the same smoke-trail data simply by changing the averaging process. This profile is similar to the one that would have been measured by a balloon if it were capable of sensing the wind over the entire altitude range in the same time as the smoke trail. The short wavelength wind variations have been filtered out, although the gross wind motion remains.

This method of measuring detailed wind profiles has several advantages. First of all, since it uses precision photographic equipment, it is very accurate. (An estimate of rms error appears in Ref. 8 and, for a typical setup, is less than $\frac{1}{2}$ fps over the altitude range of interest.) Since horizontal wind velocities can be measured in altitude increments of less than 100 ft, gust wavelengths of importance to all vehicles in the foreseeable future can be obtained. The technique can be used to measure winds acting on a particular launch vehicle by equipping the vehicle with a small smoke generator. It is also suited for use with a relatively inexpensive sounding-rocket system for collecting routine wind data.

The principal disadvantage of the smoke-trail method is its current restriction to use on clear days with good visibility conditions. However, profiles having peak wind speeds as high as 300 fps in the jet stream region have been measured by the method.

Analysis

The response of a launch vehicle to some of the wind profiles just discussed has been determined using equations and a digital computer program developed by V. L. Alley of Langley Research Center. The equations are derived for small perturbations in the pitch plane about a zero-lift reference trajectory as indicated in Fig. 6. The degrees of freedom included in the equations are translation normal to the reference trajectory, pitching, and three elastic bending modes. The coefficients of these equations vary with time due to changing mass and aerodynamic properties. Aerodynamic forces and moments are based on normal force distributions along the vehicle axis and the local time-dependent angle of attack. Penetration of the vehicle into the wind is neglected. A closed-loop attitude and attitude-rate control system, including structural feedback and a stabilizing filter network, also is represented by the equations.

The wind responses to be shown are those of a Scout four-stage, solid propellant vehicle. The Scout lifts off under about 3 g acceleration, and the maximum dynamic pressure is about 3000 psf. It has both thrust vector and aerodynamic control obtained from jet vanes and movable fin tips. The basic vehicle is aerodynamically stable and has a controlled pitch frequency of about 1 cps. The first bending frequency

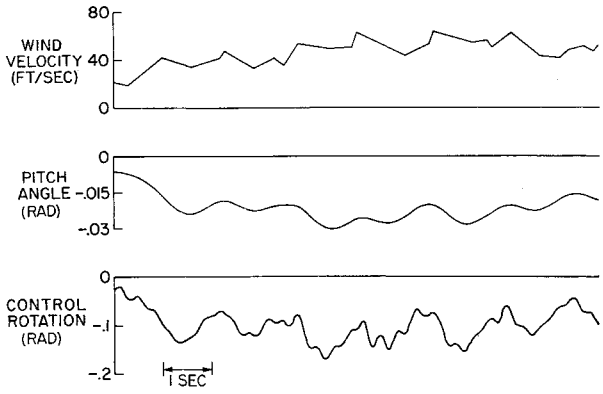

Fig. 7 Typical time histories of pitch angle and control rotation angle for flight through an α-vane-measured wind profile

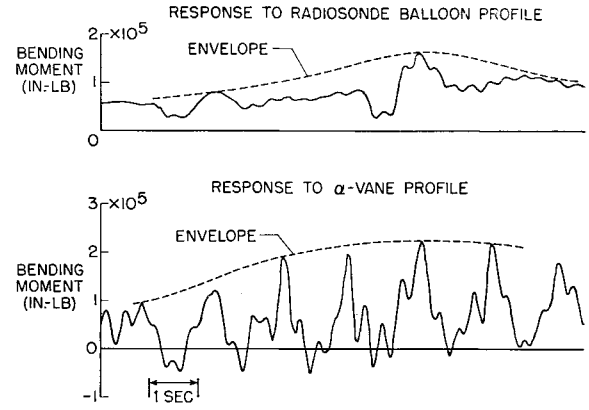

Fig. 8 Typical bending-moment time histories for flight through an α-vane-measured profile and the equivalent radiosonde-measured profile

of the vehicle is about 3 cps. All elastic modes were assumed to have damping equivalent to 2% of critical.

Results of Wind Response Studies

The Scout vehicle has been flown analytically through eight detailed wind profiles. Four profiles were obtained by the α-vane method over the years 1955 to 1960. The remaining four profiles were measured by the smoke-trail method during 1959 to 1961. The vehicle also was flown through a balloon-measured profile or a smoothed profile in each case.

α-Vane Measured Profiles

Response time histories

Typical time histories of vehicle response to the detailed, α-vane measured profile previously illustrated are shown in Fig. 7. On the upper curve the input wind velocity is shown as a function of time. This measured profile has been converted from an altitude to a time base using the reference trajectory for this particular launching. The wind input to the program is a series of points vs time, connected by straight lines between the points. For the portion of the flight illustrated, the winds never exceed about 70 fps. The middle curve is the pitch angle perturbation of the complete vehicle. Lightly damped low-frequency oscillations of the rigid-body stability mode at about 1 cps are excited by the wind and are very apparent. The bottom curve is the rotation angle of the jet vanes and the aerodynamic fin tip controls. A control angle with the same sign as the pitch angle produces a restoring moment on the vehicle. The low-frequency stability mode frequency at 1 cps also is predominant in the control angle. However, oscillations at about 3 cps, corresponding to the first elastic bending mode, show that the detailed wind profile is exciting the structural modes of the vehicle and is being sensed by the control system via the mechanism of structural feedback.

The loads experienced by the vehicle are illustrated by the time histories in Fig. 8. The bending-moment response is shown for two wind profiles—at the bottom is the response to the same α-vane profile used in Fig. 7, and at the top is the response to a radiosonde balloon profile measured at approximately the same time. The bending moment shown here and in subsequent figures is at an interstage station on the vehicle near the location of maximum bending moment. It is recognized that the exact nature of the bending-moment response will vary with vehicle station because of the influence of the various bending modes. However, only this one station will be examined in order to simplify the comparisons to be made. The oscillatory nature of the bending-moment response is very apparent. The detailed profile has caused a considerable increase in first-mode excitation, compared to the balloon profile, but it also has increased the response of the low-damped stability mode considerably near 1 cps. If an envelope of the maximum bending moments were drawn about these responses, as indicated on Fig. 8, the load levels due to the detailed profile generally would be higher than the load levels due to the balloon-measured profile.

Bending-moment envelope

The bending-moment envelopes for the responses just illustrated are shown in Fig. 9. The bending moments have been normalized by the limit bending moment at the same station and are plotted over the altitude range from launch to about 50,000 ft. One curve is shown for the detailed α-vane-measured profile and another for the radiosonde-measured profile. For most altitudes, the detailed profile produces larger loads. The maximum moment induced on the structure by the radiosonde profile occurs in the 25,000- to 30,000-ft-altitude range and equals the detailed profile moments in this region. However, the α-vane profile produces greater loads at other altitudes. Its maximum occurs between 30,000- and 35,000-ft altitude and is about 15% greater than the maximum moment produced by the radiosonde profile. Most of this increase in bending moment comes from the excitation of the elastic modes by the detailed profile. However, at the lower altitudes, it has been shown that the detailed profile also excites the lightly damped pitching mode of this vehicle which increases the load. The bending moments that result from flying these profiles never exceed about 37% of limit load, reflecting the fact that these are relatively low winds with a peak velocity of about 115 fps.

Smoke-Trail Measured Profiles

Bending-moment responses similar to those just discussed for α-vane profiles are found for wind profiles determined by the smoke-trail method. A typical example of response to a smoke-trail profile (not the profile illustrated in Fig. 5) is given in Fig. 10. The envelope of the ratio of bending moment to limit bending moment at the same station is given as a function of altitude. Envelopes are given for loads resulting from both smoke-trail and averaged smoke-trail data. These data are for a case with a large wind shear in the maximum dynamic-pressure region with very little gustiness imposed on the shear. At lower altitudes, the smoke-trail data show considerable short wavelength variation in wind velocity. This is reflected in the bending-moment envelopes by the increase in detailed profile loads, compared to the smoothed profile loads, at lower altitudes and only a slight increase, about 5%, in the peak wind region. Notice that the maximum bending moment is only about

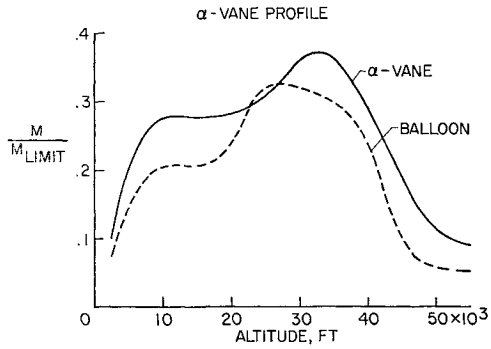

Fig. 9 Bending-moment envelopes for an α-vane-measured profile and its equivalent balloon-measured profile; maximum V_w = 115 fps

30% of the limit load. Again, this results from the low peak wind velocities of about 115 fps.

Bending-Moment Amplification by Detailed Profiles

The bending-moment envelopes just discussed have shown that the detailed profiles generally produce higher loads than the balloon-type profiles. The actual amplification of the bending moment at various altitudes is illustrated in Fig. 11 for three wind measurements. The bending-moment envelope of the detailed profile has been divided by the envelope of bending moment for the smoothed profile, such that, at any altitude, the ordinate gives the increase in load produced by the detailed profile. All three profiles and peak wind velocities of about 115 fps such that maximum steady wind loads would be comparable. The amplification by the detailed profiles at various altitudes is seen to vary drastically with the particular case, illustrating the dependence of the load on the details of the profile. Not only does the amplification of the load depend on the details of the particular profile, but also it depends on the characteristics of the particular vehicle being considered. (In addition, this factor will reflect any changes in wind velocity which occur between the time of the detailed and the balloon measurements.) The large amplifications shown here do not necessarily endanger this vehicle, since it has been designed for a much higher peak wind with an added margin for gusts. Also, some of the largest amplifications occur in the low- or high-altitude regions, where dynamic pressure is reduced, so that total loads are within design limits.

The increase in bending moments which results from using the detailed profiles instead of the smoothed or averaged profiles generally can be credited to the short wavelength fluctuations, or "gustiness," of the detailed profiles. However, high gross winds and large gusts do not necessarily occur at the same time. Thus, it can be argued that, since most of the detailed wind profiles have been measured on relatively low wind days, the amplification of bending

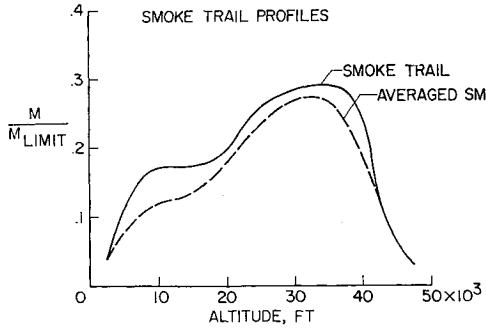

Fig. 10 Bending-moment envelopes for a smoke-trail profile and its averaged profile; maximum V_w = 114 fps

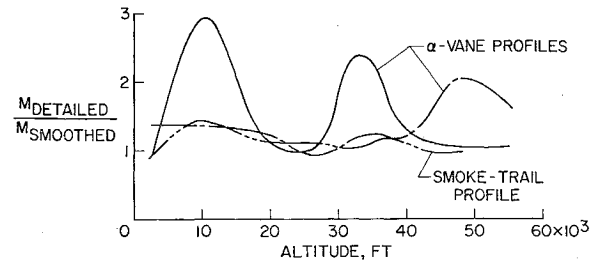

Fig. 11 Bending-moment amplification as a function of altitude for three wind soundings having maximum V_w of about 115 fps

moment by the detailed fluctuations of these profiles may exaggerate the effect to be expected on high wind days. Figure 12 is an attempt to establish the trend of the bending-moment amplification as the peak wind velocity increases. The ratio of the maximum bending moment resulting from the detailed profiles to the maximum bending moment resulting from the smoothed profiles is plotted against the peak wind velocity of the detailed profile. The bending moments presented are those that occur in the maximum dynamic-pressure portion of the launch trajectory. The circles indicate profiles obtained by the smoke-trail method, and the squares indicate profiles measured by the α-vane method. Considerable scatter is evident in these points, but a trend does appear to be indicated. Larger amplifications occur at low peak wind velocities, whereas continually decreasing amplifications occur as the peak wind velocity increases. The scatter evident here is partially due to the difficulty of obtaining radiosonde balloon data at the same time as the detailed profile measurement. From 30 min to 5 hr time difference exists in these soundings, providing time for the wind profile to have changed. Of course, much of the scatter simply is due to the dependence of the bending-moment response on the details of the particular profile and the particular vehicle. For instance, the α-vane profile that produces amplifications greater than 2 for a peak wind velocity of 117 fps was a particularly "gusty" profile. However, Fig. 12 does seem to indicate that detailed wind profiles with very high peak winds will amplify the bending moments produced by the smoothed profiles by only moderate amounts.

Many additional data are needed. The variations in bending moment which result from response to the various profiles indicate the importance of the characteristics of the particular profile. Considerably more experience with these profiles applied to various launch vehicles is needed before realistic design criteria using them can be established. A possible design approach would be similar to the one recommended in Ref. 5. This would be a brute force method in which samples of measured, detailed wind profiles (possibly 15, 50, or 150 profiles) would be used to predict loads on a launch vehicle. Such a technique would require a massive computer program involving variable parameters and elastic degrees of freedom, but it would not necessitate separate

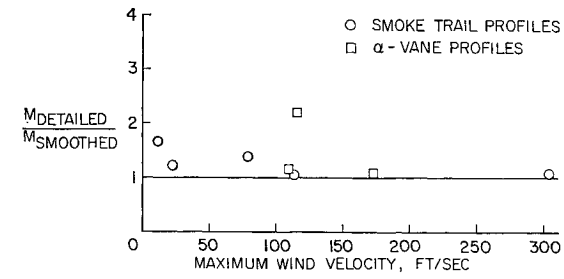

Fig. 12 Bending-moment amplification by detailed wind profiles near maximum dynamic pressure

consideration of winds and gusts. A more sophisticated approach would be the use of a statistical method such as proposed in Refs. 13 and 14. However, until more detailed wind data are available and the advantages of the refined design procedures are established, relatively simple approaches involving a synthetic wind profile plus discrete gusts undoubtedly will continue to be used by industry.

Concluding Remarks

Detailed wind profiles obtained by two methods have been discussed. The two methods of measuring horizontal wind velocity as a function of altitude, the α-vane method and the smoke-trail method, use an angle-of-attack measuring device carried by a launch vehicle and a trail of smoke left by a sounding rocket, respectively, to sense the motion of the atmosphere. A launch vehicle has been flown analytically through a number of these detailed profiles as well as equivalent balloon-measured or smoothed profiles. The detailed wind profiles were shown to excite the pitch and elastic bending modes of the vehicle and, as a result, to produce higher loads on the vehicle structure than are produced by balloon-type wind profiles. Present design procedures (which are based on balloon-measured profiles) allow for this increased load by adding a somewhat arbitrary gust load to the wind load. When more of the detailed wind profile data are available, revision of design procedures to include the detailed variations in the winds would seem to be indicated.

References

[1] Sissenwine, N., "Windspeed profile, windshear, and gusts for design of guidance systems for vertical rising air vehicles," Air Force Surveys in Geophys. **57** (AFCRC-TN-54-22), Air Force Cambridge Research Center (November 1954).

[2] Sissenwine, N., "Development of missile design wind profiles for Patrick AFB," Air Force Surveys in Geophys. **96** (AFCRC-TN-58-216, ASTIA Doc. AD-146 870), Air Force Cambridge Research Center (March 1958).

[3] Hobbs, N. P., Criscione, E. S., Mazzola, L. L., and Frassinelli, G. J., "Development of interim wind, wind shear, and gust design criteria for vertically-rising vehicles," Avidyne Research Inc., Wright Air Dev. Div. TR 59-504(AD-316 913) (July 1959).

[4] Scoggins, J. R. and Vaughn, W. W., "Cape Canaveral wind and shear data (1 through 80 km) for use in vehicle design and performance studies," NASA TN-D 1274 (1962).

[5] Mazzola, L. L., Hobbs, N. P., and Criscione, E. S., "Wind, wind shear, and gust design criteria for vertically-rising vehicles as recommended on the basis of Montgomery, Alabama, wind data," Wright Air Dev. Div. TR 61-99 (1961).

[6] Donely, P., "Summary of information relating to gust loads on airplanes," NACA TR 997 (1950).

[7] Pratt, K. G. and Walker, W. G., "A revised gust-load formula and a re-evaluation of *V-G* data taken on civil transport airplanes from 1933 to 1950," NACA TR 1206 (1954).

[8] Press, H. and Steiner, R., "An approach to the problem of estimating severe and repeated gust loads for missile operations," NACA TN 4332 (1958).

[9] Reisig, G. H. R., "Instantaneous and continuous wind measurements up to the higher stratosphere," J. Meteorol. **13**, 448–455 (October 1956).

[10] Tolefson, H. B. and Henry, R. M., "A method of obtaining detailed wind shear measurements for application to dynamic response problems of missile systems," J. Geophys. Research **66**, 2849–2862 (1961).

[11] Henry, R. M., Brandon, G. W., Tolefson, H. B., and Lanford, W. E., "The smoke-trail method for obtaining detailed measurements of the vertical wind profile for application to missile-dynamic-response problems," NASA TN D-976 (1961).

[12] Leviton, R., "A detailed wind profile sounding technique," *Proceedings of the National Symposium on Winds for Aerospace Vehicle Design* (Air Force Surveys in Geophys. **140**, AFCRL-62-273(I), March 1962), Vol. I, pp. 187–195.

[13] Trembath, N. W., "Control system design wind criteria," Space Technology Labs. GM-TM-0165-00258 (June 30, 1958).

[14] Bieber, R. E., "Missile structural loads by nonstationary statistical methods," J. Aerospace Sci. **28**, 284–294 (1961).

See December 1962 ARS Journal, page 1845, for further details